A SHADOW MASK-EVAPORATED TOPSIDE PYROMEMS IGNITER

D.A. de Koninck, D. Briand, and N.F. de Rooij
Ecole Polytechnique Fédérale de Lausanne (EPFL), Institute of Microengineering (IMT),
The Sensors, Actuators and Microsystems Laboratory (SAMLAB), Lausanne, Switzerland

Abstract: A shadow mask-evaporated pyroMEMS igniter is presented. The metallization was successfully carried out without ignition or any visible degradation of the propellant charge during evaporation. Directly depositing the Joule-heating igniter onto the propellant charge led to a high level of ignition delay time homogeneity (< 1 ms st. dev.) as well as smooth combustion behavior. Effect of different deposition thicknesses (500 nm vs. 2000 nm), deposition methods (e-beam vs. thermal) and substrate holders (rotary-planetary vs. line-of-sight) on ignition behavior were investigated. Two different ignition regimes were observed depending on input power and igniter thickness: Joule-heating and spark-induced ignition. Highest fabrication repeatability (in terms of electrical resistance) and ignition reliability (in terms of ignition delay time) were obtained with the 2000 nm thick igniters.

Keywords: Igniter, Micro-Combustion, PyroMEMS, Solid Propellant

INTRODUCTION

PyroMEMS, or pyrotechnical micro-electro-mechanical systems, are a class of fuel-based microsystems that use solid propellants to generate high-pressure, high-temperature gaseous products. PyroMEMS have gained interest recently as a simple, low-cost source of on-chip pressurized gas. Potential applications include gas generators for micro-fluidic devices [1], pyrotechnic switches [2] and micro-thrusters for small satellites [3].

. The main problem with the pyroMEMS devices developed to date is poor ignition reliability due to inconsistent thermal/mechanical contact between the ignition source and propellant charge [4]. Rossi et al. [3] reported large dispersion (from 30-750 ms) in ignition delay times due to unreliable fuel/igniter thermal contact—ostensibly caused by their fuel deposition technique. Others simply do not report on the ignition reliability of their devices (e.g., [5]). Tanaka et al. [6] attempted to overcome the contact problem by using a non-contact spark igniter; however, it failed to ignite the fuel. Last year, de Koninck et al. [7] presented a bottomside pyroMEMS igniter which achieved reliable fuel ignition and combustion; however, the method was very sensitive to the igniter/propellant alignment and was limited to fuel drops—as opposed to filled chambers.

The igniter presented herein overcomes the thermal contact problem by directly patterning the igniter onto the propellant surface via shadow mask evaporation. This method is compatible with both fuel drops as well as full chambers.

This communication will outline the fabrication, characterization and testing of the igniters.

CONCEPT AND FABRICATION

The pyroMEMS igniter consisted of either a propellant-filled cylindrical cavity or a fuel drop-coated substrate with a shadow mask-evaporated heater deposited overtop. The propellant used in this study consisted of a mixture of an energetic material, polymeric binder and solvent—which evaporated after the deposition yielding a solid propellant mass. The fuel surface roughness was typically on the order of 10 μm.

The pyroMEMS igniters were fabricated via shadow mask evaporation. The shadow mask consisted of a 100 μm thick stainless steel sheet patterned via laser micromachining. A 500 μm stainless steel spacer was used to prevent the shadow mask from touching the fuel drop. Fuel-coated glass substrates were from a previous study [7] were used to fabricate the devices. Deposition thickness, deposition method (and material) and substrate stage were varied in order to optimize the igniter performance (see Table 1). 20 igniters were fabricated in each trial for a total of 80 igniters.

Table 1: Evaporation parameters

#	Method	Thickness	Substrate Holder
1	E-beam (Al)	500 nm	Rotary-planetary
2	Thermal (Ag)	500 nm	Rotary-planetary
3	E-beam (Al)	2000 nm	Rotary-planetary
4	E-beam (Al)	500 nm	Line-of-Sight

The baseline case (trial #1) consisted of a 500 nm (nominal) aluminum film deposited via electron-beam evaporation on a rotary-planetary stage. Aluminum was chosen for its low heat of vaporization in order to minimize the energy of the impinging ions and

prevent potential damage to or ignition of the propellant during evaporation. The rotary-planetary stage was used to obtain conformal coverage of the rough fuel surface to achieve a continuous metal line, but at the cost of poorer feature definition and thinner metal lines.

The three alternate trials each modified one of these three parameters to determine their relative importance with respect to igniter performance. For the thermal evaporation trial, silver rather than aluminum was deposited for lack of a suitable aluminum source and because of its excellent adhesion properties with glass. For trial #3, the metal thickness was increased to 2000 nm (nominal). Unfortunately, the line-of-sight trial yielded igniters with poor substrate adhesion and the devices were discarded.

IGNITER CHARACTERIZATION

Evaporation of metal onto an energetic material was successfully carried out without ignition or any other visible degradation of the propellant (e.g., Figure 1). The different pyroMEMS igniters were characterized visually and by measuring their electrical resistance. For the igniters fabricated using the rotary-planetary substrate holder (Figure 1), the igniter narrowed more or less at the apex of the fuel drop—depending on its height—due to the different gaps between the fuel surface and the shadow mask.

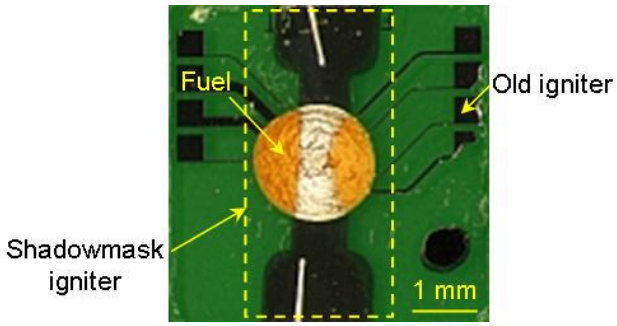

Figure 1: Dark field micrograph of a 500 nm thick, E-beam evaporated, aluminum igniter deposited on glass substrates using a rotary-planetary substrate holder. The shadow mask igniter is the vertical dog-bone shape running overtop the orange fuel drop. The contact pads lining the sides of the chips and interconnects leading underneath the fuel drops are the igniters from [7] and are unrelated to the present study (indicated as "old igniter").

The median resistance values and standard deviations of the igniters are given in Table 2. The trial identifiers refer to the parameter which was varied during that trial, as highlighted in Table 1. The baseline trial igniter resistances exhibited relatively large scatter due to their small thickness as compared to the propellant surface roughness (~10 μm). Not only did increasing the metal thickness by a factor of 4 resulted in a likewise decrease in resistance (5.34 vs. 1.45 Ω), but also greatly decreased the observed scatter in resistance values (9.55 vs. 0.21 Ω). The 500 nm silver igniters suffered from the same problem as the 500 nm aluminum igniters: large scatter due to the high surface roughness of the fuel drops.

Table 2: PyroMEMS igniter resistance

#	Trial ID	Median (Ω)	Std. Deviation (Ω)
1	Baseline	5.34	9.55
2	Thermal (Ag)	15.8	242
3	2000 nm	1.45	0.21
4	Line-of-Sight	—	—

IGNITION SETUP

A 100-millisecond, square voltage pulse was applied to the igniters using a function generator (HP33120A) coupled to a high-speed power amplifier (NF Electronic Instruments 4015). The voltage pulse magnitude was varied from 2 to 100 V. Two high-speed digital multimeters (Agilent 34411A) measured the voltage and current passing though the igniter during the pulse. Simultaneously, a high-speed framing camera (Vision Research Phantom v210) mounted onto a stereomicroscope acquired images of the combustion process at up to 10,000 frames per second. All of the measurement devices were computer controlled via GPIB connectors using a custom MATLAB script.

RESULTS AND DISCUSSION

Two different ignition regimes, Joule-heating and spark-induced, were observed depending on the thickness of igniter and the input power level.

The Joule-heating ignition regime was characterized by a well defined ignition delay time, which decreased with increasing input power. Combustion began with the formation of one or more flame kernels—which ruptured the igniter—and steady flame spreading until the fuel drop was completely consumed (see Figure 2).

A so-called spark-induced ignition was said to occur when the ignition was preceded by a spark above the igniter. The sparks always occurred within one high-speed video frame (i.e., less than 100 μs) of the initiation of the voltage pulse (see Figure 3). They tended to appear in the troughs (darkened zones) of the igniter surface—i.e., where breaks and discontinuities were likely to occur. Sparks also

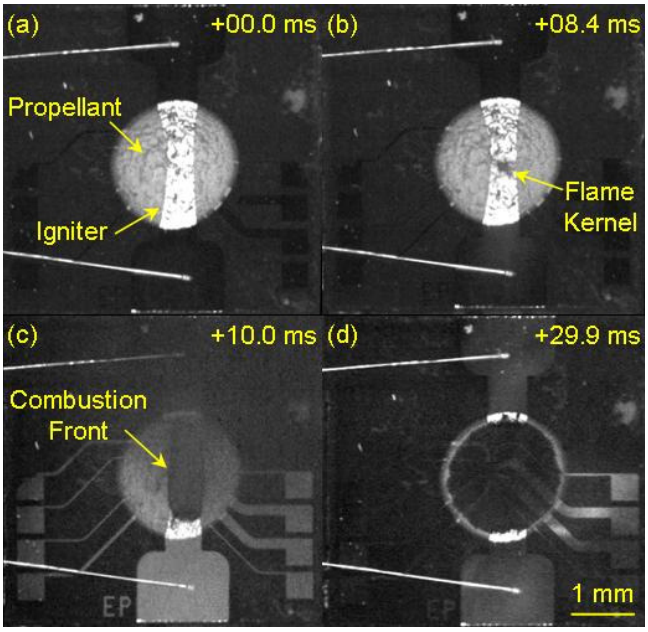

Figure 2: High-speed video frames of a 2000 nm thick aluminum igniter undergoing Joule-heating ignition (mean input power = 1.7 W): (a) before ignition, (b) appearance of flame kernel, (c) flame spreading and peeling of igniter, and (d) post combustion. Time stamp is given relative to start of voltage pulse.

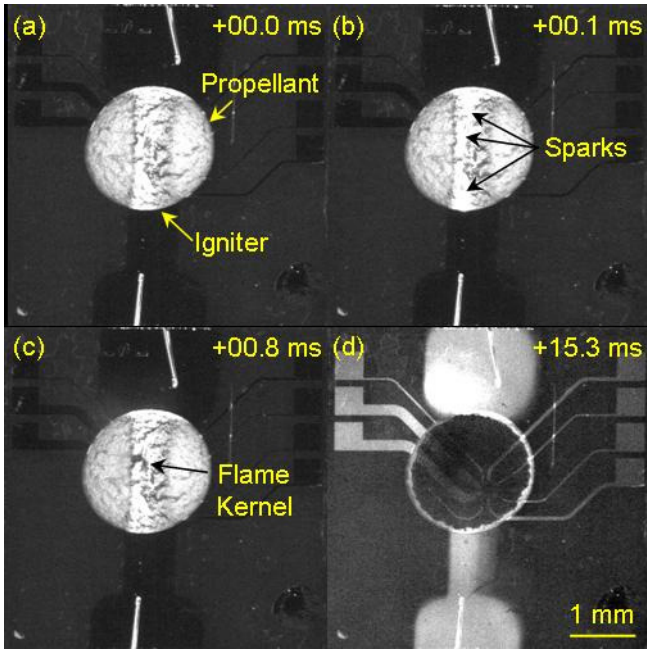

Figure 3: High-speed video frames of a 500 nm thick silver igniter undergoing spark-induced ignition (mean input power ~ 30 W): (a) before ignition, (b) appearance of sparks, (c) flame kernel formation, and (d) post combustion. Time stamp is given relative to start of voltage pulse.

appeared around the igniter contact pad/bondwire interface—i.e., zones in the contact pad weakened by wire bonding (see Figure 7).

For the 2000 nm thick igniters, all 20 igniters were successfully ignited. Typical voltage and current traces are given in Figure 5 showing a smooth decrease in current due to the increase in temperature with time prior to ignition. When the fuel ignited, the current dropped to zero as the igniter was severed. As such, the igniters automatically minimized the input energy needed to achieve ignition for a given input power level. The Joule-heating ignition regime was observed at moderate input powers—between 1.7 and 11.3 W (see Figure 4). At lower input powers (0.87 W and below), no combustion occurred for voltage pulses up to 2.5 s (i.e., 2 orders of magnitude longer than the longest ignition delay times reported in Figure 4). For higher powers (~30 W), spark-induced ignition was observed. Mean ignition delay times as well as delay time variability (st. dev.) were both found to decrease exponentially with increasing input power.

The thin igniters (whether aluminum or silver) failed to ignite at the moderate input powers in which Joule-heating ignition was observed; rather, only spark-induced ignition was seen and only at large input powers (75-100 V, or ~15-20 W). 30 % (12/40) of the thin igniters were successfully ignited via spark-induced ignition. For a further 15 devices, the fuel was successfully ignited, but the igniters were completely destroyed—i.e., evaporation of the igniter metal and bondwires (see Figure 6) was observed. Finally, the 13 remaining devices generated sparks, but failed to ignite the propellant charge (see Figure 7).

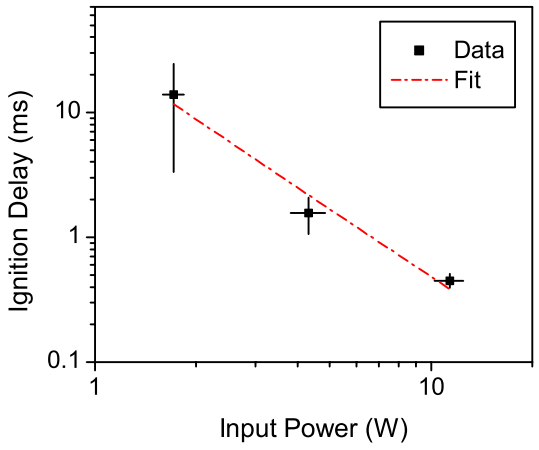

Figure 4: Ignition delay time vs. input power for the 2000 nm thick igniters. Each data point represents the mean of 4 separate trials.

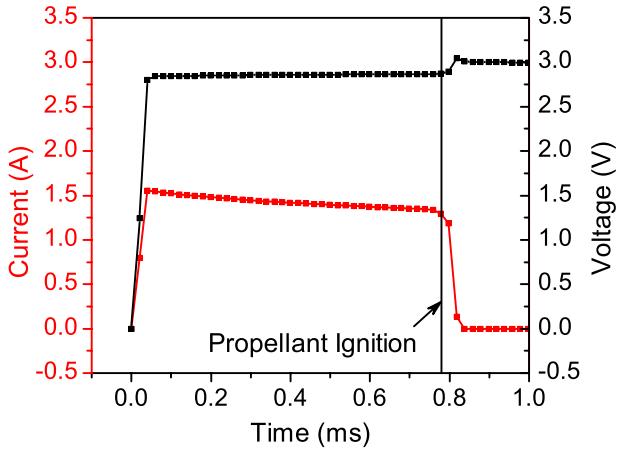

Figure 5: Representative current and voltage traces for a 2000 nm thick aluminum igniter (input power = 4.1 W).

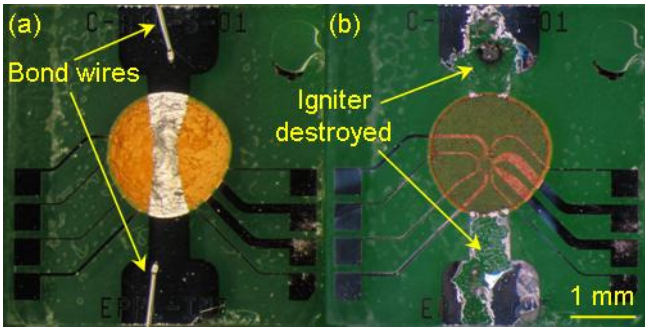

Figure 6: Before and after micrographs of a 500 nm thick aluminum igniter that was destroyed by voltage pulse.

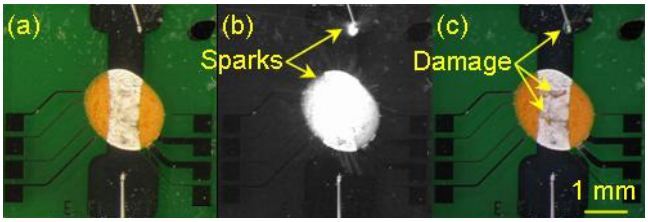

Figure 7: Micrographs of a 500 nm thick aluminum igniter that failed to ignite due to spark-induced igniter damage: (a) before, (b) during and (c) after voltage pulse.

CONCLUSION

This communication presented the fabrication, characterization and testing of a shadow mask evaporated pyroMEMS igniters. A preliminary process-parameter study indicated that igniter thickness was the critical parameter to achieving reliable, Joule-heating igniters. Igniter delay time variability of less than 1 ms was achieved, which represents the lowest reported value in the literature to date. Future work will include further exploration of the processing design space, demonstration of shadow mask igniters over propellant-filled cavities and mating of a nozzle to the outlet to demonstrate a full pyroMEMS thruster.

ACKNOWLEDGEMENTS

D.A. de Koninck gratefully acknowledges the financial support from the EPFL Space Center ESRP under contract #2007/033 as well as a postgraduate scholarship from the Natural Sciences and Engineering Research Council of Canada (NSERC).

REFERENCES

[1] Choi Y H, Son S U, Lee S S 2004 A micropump operating with chemically produced oxygen gas *Sensors and Actuat A-Phys* **111** 8-13

[2] Pennarun P, Rossi C, Estève D, Colin R-D 2007 Single use, robust, MEMS based electro-thermal microswitches for redundancy and system reconfiguration *Sensors and Actuators A: Physical* **136** 273-281

[3] Rossi C, Larangot B, Phuong-Quyen P, Briand D, de Rooij N F, Puig-Vidal M, Samitier J 2006 Solid Propellant Microthrusters on Silicon: Design, Modeling, Fabrication, and Testing *J Microelectromech Syst* **15** 1805-1815

[4] Rossi C, Estève D 2005 Micropyrotechnics, a new technology for making energetic microsystems: review and prospective *Sensors and Actuat A-Phys* **120** 297-310

[5] Lee J, Kim K, Kwon S 2010 Design, fabrication, and testing of MEMS solid propellant thruster array chip on glass wafer *Sensors and Actuat A-Phys* **157** 126-134

[6] Tanaka S, Kondo K, Habu H, Itoh A, Watanabe M, Hori K, Esashi M 2008 Test of B/Ti multilayer reactive igniters for a micro solid rocket array thruster *Sensors and Actuat A-Phys* **144** 361-366

[7] de Koninck D A, Bley U, Gass V, Briand D, de Rooij N F PyroMEMS Igniter Based on a Temperature Gradient: Concept, Fabrication and Characterization *PowerMEMS 2009 (Washington D.C., USA, December 1-4, 2009 2009)* 108-111